J Mol Model (2011) 17:81–88
DOI 10.1007/s00894-010-0651-6

ORIGINAL PAPER

Electropolymerization of 3′,4′-disubstituted 2,2′:5′,2″-terthiophene derivatives. A theoretical and photovoltaic characterization

Jorge H. Vélez · Soledad Gutiérrez-Oliva · Fernando R. Díaz · Maria Angelica del Valle · Alejandro Toro-Labbé · Jean C. Bernède · Gastón A. East

Received: 16 October 2009 / Accepted: 10 December 2009 / Published online: 8 April 2010

Abstract In the present work a series of β-substituted thiophenes have been synthesized and their electrochemical behavior studied. The products obtained by electro-oxidation are highly dependent on the substituent, affording sometimes conducting polymers, insulating layers or soluble species. This behavior has been ascribed to specific electronic and/or steric factors. Theoretical calculations at the density functional theory level confirm the experimental findings and assess the use of reactivity descriptors for modeling complex chemical systems with specific polymerization patterns. In particular, the analysis of the polymerization sites of terthiophene derivatives using the dual descriptor for chemical reactivity and selectivity allows one to predict the specific sites able for reaction and explains correctly the observed polymerization pattern.

Keywords Conducting polymers · Conjugated polymers · Electropolymerization · Heteroatom-containing polymers

J. H. Vélez · F. R. Díaz · M. A. del Valle · G. A. East
Laboratorio de Polímeros, Facultad de Química,
Pontificia Universidad Católica de Chile,
Vicuña Mackenna 4860, Casilla 306, Correo 22,
Santiago, Chile
e-mail: jhvelez@uc.cl

S. Gutiérrez-Oliva (✉) · A. Toro-Labbé
Laboratorio de Química Teórica Computacional (QTC),
Facultad de Química, Pontificia Universidad Católica de Chile,
Vicuña Mackenna 4860, Casilla 306, Correo 22,
Santiago, Chile
e-mail: msg@uc.cl

J. C. Bernède
LPSE,
2 rue de la Houssiniére BP 92208,
443220 Nantes Cedex 3, France

Introduction

In the past few years research about heterocyclic conductive polymers, chemically or electrochemically synthesized, has been particularly intensified [1, 2]. Among heterocyclic polymers, polythiophenes have been largely studied owing to their potential utility as organic materials for the assembling of diverse electric or electronic devices [2–7], since besides their electrical and optical properties, they possess excellent environmental stability [1, 8–11]. Hence, their current applications are varied: organic cells, electrochromic displays, chemical sensors, light emitting diodes (LED), etc. Studies of molecules, aimed at obtaining materials with specific properties, have aroused great interest starting from preparations and modifications that enable addition of different functional groups, easily tuning electrical, optical, and magnetic properties. Our interest is focused upon synthesis and electronic structure analysis of thiophene derivatives, namely 3′,4′-disubstituted 2,2′:5′,2″-terthiophene (Fig. 1), their electrochemical features and its polymerization, as well as their spectral characteristics, oxidation potentials, and likely prospective applications in photocell assembling. In this context, computational quantum chemistry methods are well suited to model such systems. Moreover, specific features exhibited by the electronic density may direct the design of new materials, these features can be shaped through the use of reactivity descriptors such as chemical potential [12], hardness [13], Fukui functions [14], dual descriptor for chemical reactivity and selectivity [15, 16].

Experimental and theoretical methods

Experimental methods

FT-IR spectra were recorded on a Perkin–Elmer, model 1710-FT, spectrometer, by solid dispersion with KBr

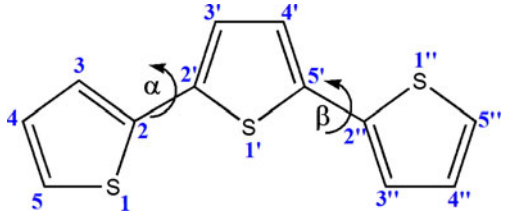

Fig. 1 Molecular structure and numbering of atoms of the 2,2′;5′,2″-terthiophene molecule. α and β are the torsional angles formed by planes of the rings of thiophene. The *trans* conformers correspond to torsional angles of 180°

pellets. ^{1}H and ^{13}C NMR spectra were run on a Bruker 200P Spectrometer, in $CDCl_3$ with TMS as the internal standard. Microanalyses were made on a Fison EA 1108 microanalyzer. Scanning electron microscopy (SEM) micrographs were recorded on a high-resolution SEM (Jeol 6400 F).

Monomers were synthesized following methods described in the literature [17–19] using a transition metal-catalyzed cross-coupling of a Grignard reagent with organic halides. Electrochemical synthesis and characterization were performed in a three-compartment, three electrode cell utilizing a Voltalab PGZ100 (Radiometer) potentiostat and anhydrous dichloromethane as solvent.

Monomer electropolymerization was accomplished by either potentiodynamic sweeps (CV) or potentiostatic steps. The working electrode was a Pt polycrystalline disc (0.07 cm^2 geometric area). All potentials quoted in this paper are referred to a Ag/AgCl electrode in tetramethylammonium chloride that matches the potential of a SCE at room temperature [20].

Theoretical methods

Chemical potential (μ), the negative of the electronegativity ($\mu = -\chi$), and chemical hardness (η) are among the most important global properties aimed at describing chemical reactivity. Within the framework of density functional theory (DFT), the chemical potential and hardness for an N-electron system with total energy E and external potential υ((r) are defined as follows: [12, 13]:

$$\mu = \left(\frac{\partial E}{\partial N}\right)_{\upsilon(r)} = -\chi; \quad \eta = \left(\frac{\partial^2 E}{\partial N^2}\right)_{\upsilon(r)}. \tag{1}$$

Physically, the chemical potential characterizes the escaping tendency of electrons from equilibrium and the molecular hardness can be seen as a resistance to charge transfer [21]. The inverse of the hardness is the softness: $S = 1/\eta$ and can be used to complement the observations made through chemical potential and hardness. In the present case, the above defined properties will be used to characterize specific isomers from a reactivity viewpoint.

In numerical applications, μ and η are calculated by the following approximate equations based upon the finite difference approximation and Koopman's Theorem [22, 23]:

$$\mu \approx \frac{1}{2}(\varepsilon_L + \varepsilon_H); \quad \eta \approx \frac{1}{2}(\varepsilon_L - \varepsilon_H) \tag{2}$$

where ε_H and ε_L are the energies of the highest occupied and the lowest unoccupied molecular orbitals, HOMO and LUMO, respectively. Ionization potential (I) and electron affinity (A) are related to the orbital energies through the Koopman's Theorem: $I = -\varepsilon_H$; $A = -\varepsilon_L$.

In order to identify the reactive sites toward electrophilic and nucleophilic attacks, a variety of indexes, relatively suited to specific situations, exist [21, 24]. In this particular case we propose the use of local reactivity descriptors like the Fukui function $f(r)$ that are necessary for explaining site selectivity in a molecule. The Fukui function is defined as [14]:

$$f(r) = \left(\frac{\delta\mu}{\delta\upsilon(r)}\right)_N = \left(\frac{\partial\rho(r)}{\partial N}\right)_{\upsilon(r)}. \tag{3}$$

Owing to the discontinuity of the derivative of Eq. 3, two different Fukui functions can be defined by applying the finite difference approximation [21]:

$$f^+(r) = \left(\frac{\partial\rho(r)}{\partial N}\right)^+_{\upsilon(r)} \approx \rho_L(r); \quad f^-(r) = \left(\frac{\partial\rho(r)}{\partial N}\right)^-_{\upsilon(r)} \approx \rho_H(r). \tag{4}$$

At point r, $f^+(r)$ measures the reactivity toward a nucleophilic attack that results in an electron increase in the system [21, 25, 26] whereas $f^-(r)$ measures the reactivity toward electrophilic attacks which results in an electron decrease in the system [21, 25, 26]. Toro-Labbé and co-workers [15] have recently proposed a dual descriptor, $\Delta f(r)$, for a simultaneous identification of nucleophilic and electrophilic sites within a molecular system. The dual descriptor for chemical reactivity and selectivity is defined as the derivative of molecular hardness with respect to the external potential and can be expressed as the difference between the already defined nucleophilic and electrophilic Fukui functions:

$$\Delta f(r) = \left(\frac{\delta\eta}{\delta\upsilon(r)}\right)_N = \left(\frac{\partial f(r)}{\partial N}\right)_{\upsilon(r)} \cong [f^+(r) - f^-(r)] \cong [\rho_L(r) - \rho_H(r)] \tag{5}$$

If $\Delta f(r)>0$, then the site r is favored for a nucleophilic attack, whereas if $\Delta f(r)<0$, then the site may be favored for an electrophilic attack. Therefore, positive values of $\Delta f(r)$ identify electrophilic regions within the molecular topology, whereas negative values of $\Delta f(r)$ define nucleophilic regions. Through these descriptors it will be possible to identify the reactive sites of the monomers and characterize the preferred polymerization sites.

Computational details Theoretical calculations using the *Gaussian03* [27] program were performed to help rationalize the experimental data. With this purpose the electronic structure of 2,2′:5′,2″-terthiophene and 3′,4′-disubstituted derivatives have been characterized using DFT [28, 29] with the B3LYP hybrid functional, a combination of Becke non local exchange functional and Lee-Yang-Parr (LYP) correlation functional [30]. Energies listed in Table 2 are referred to the more stable isomer (*cis* and *trans*) of each couple of molecules.

Results and discussion

Experimental results

Electropolymerization processes Thiophene potentiostatic electropolymerization is hindered by the need of applying large oxidation potentials. According to data quoted in the literature, thiophene oxidation potential is 1.80 V, higher than other heterocyclic monomers such as pyrrole, whose oxidation occurs at 0.8 V. This is consistent with the fact the oxidation potential increases with electronegativity of the heteroatom. On the other hand, this potential decreases as conjugation increases, e.g., terthiophene, molecule chosen for analysis and discussion in the present survey that would correspond to a trimer of thiophene. Here the effect of 3′ and 4′ substituents on nucleation and growth, oxidation potential, deposit morphology, conductivity, and utility in electrochemical devices are considered.

For the sake of comparison, the same concentration of each monomer was used and, owing to the low solubility of the synthesized monomers (1×10^{-2}M), identical concentration of supporting electrolyte (1×10^{-2}M) was selected, (monomer: supporting electrolyte=1:1) so that it may compete with monomer's solubility, i.e., decreasing its solubility even further.

Electrodynamic polymerization was accomplished using 50 mV s^{-1} scan rate. This sweep rate is too high and capacitive current becomes an important fraction of the total current causing distortion of the voltammogram. On the other hand, this scan rate, shows no other unwanted drawbacks were found. Table 1 shows the obtained results.

Several characteristics related to the capacity of heterocyclic monomers, depicted in Fig. 2, to conduct electricity have been reviewed in the present work. In such a context, it is desirable that, besides low ionization potential and high electronic affinity that facilitate doping, polymers possess a nearly planar structure and a small band-gap value. ^{1}H NMR spectra showed that 3,3″ protons in system **5** shift toward low fields, 7.59 ppm, as a result of the proximity of electron acceptor (nitro) groups, particulary in the *cis* configuration **5a**, unshielding and bringing it to lower fields, compared to the equivalent proton of other synthesized monomers, e.g., 3′4′-diphenyl 2,2′:5′,2″ terthiophene (**4**) which is not so strongly affected and is observed at higher fields, Th-H3, Th-H3″, δ=7.03 ppm.

The obtained results are consistent with those previously reported for thiophene electropolymerization in various working conditions [2–5], and they are unable to show, under specific experimental conditions (solvent, monomer and/or electrolyte concentration, etc.), that a particular contribution, as a function of electrolysis time and working potential, prevails. In this manner a certain degree of control may be exercised over the morphology of the deposit to be obtained. Waltman et al. found a linear correlation between thiophene and Hammet substituted thiophene oxidation potential [31, 32], this shows that electronic effects drastically influence the reactivity on the thiophene ring [31, 32]. Consequently, monomers substituted by electron acceptor groups, e.g., 3′4′-dinitroterthiophene (**5**), display oxidation potential higher than terthiophene and are difficult to electro-synthesize. On the other hand, polymerization of substituted terthiophene monomers, such as 3′,4′ dibromothiophene (**2**), needs also high oxidation potentials with respect to terthiophene and, usually, are difficult to polymerize, e.g., 3-chloro, 3-bromo, 3,4-dibromo, and 3-iodothiophenes [2], and yield low conducting polymers with high oxidation potential. However, it should be noticed that the

Table 1 Features of polymeric deposits

Monomer		Monomer		Characteristics of the respective electro-deposit		
		Molecular geometry	E_{ox}	NGM [37–44]	Morphology	Device
1b	2,2′:5′,2″-terthiophene	trans	1200	NI2D + NI·D_{ct} + $NI3D_{dif}$	Cauliflower	diode
2a	3′,4′-dibromo-2,2′:5′,2″-terthiophene	cis	1600	NI2D + NI·D_{ct} + $NI3D_{dif}$	Small spheres	diode
3b	3′-bromo-4′-thienyl-2,2′:5′,2″-terthiophene	trans	1400	NI2D + NI·D_{ct} + $NI3D_{dif}$	Small spheres	photocell
4b	3′,4′-diphenyl-2,2′:5′,2″-terthiophene	trans	1500	$NI2D_{ct}$ + $NI3D_{dif}$	Irregular	photocell
–	3′4′-dibutyl-2,2′:5′,2″-terthiophene	trans	1100	NI2D + NI·D_{ct} + $NI3D_{dif}$	Irregular coating	photocell
5a	3′,4′-dinitro-2,2′:5′,2″-terthiophene	cis	1800	NI2D + NI·D_{ct} + $NI3D_{dif}$	Regular spheres Irregular coating	–

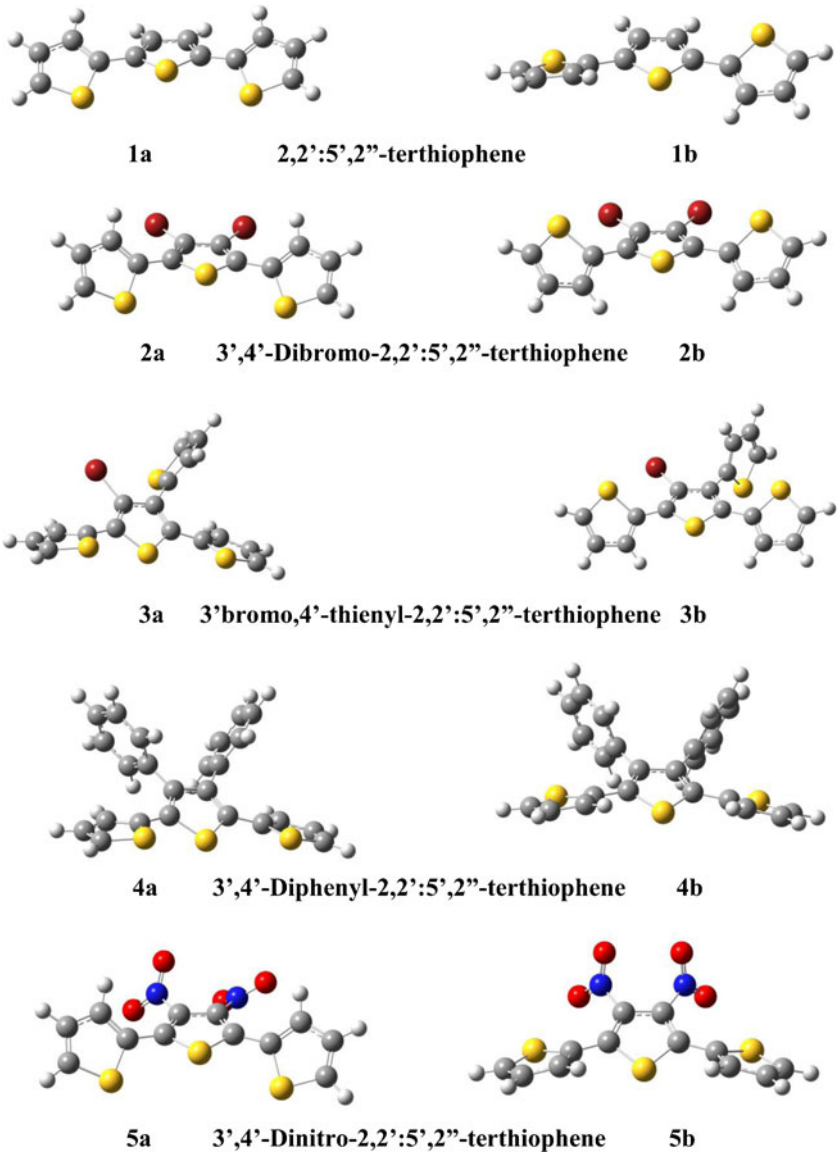

Fig. 2 Optimized molecular structure of the substituted terthiophenes investigated (*cis*- left and *trans*- right)

electrochemical response is mainly affected by the combination of two factors, electronic and steric, giving rise to failure or hindrance of the electro-polymerization. Moreover, consistency between high experimental oxidation potentials, E_{ox} (Table 1) and computed electronegativity χ (Table 2) can be observed for 3′4′-dinitroterthiophene (**5**) and 3′,4′ dibromothiophene (**2**) systems.

Although steric factors do not appreciably affect the oxidation potential of the monomer, they exercise considerable influence over the structure and characteristics of the substituted polymer and, in some extreme situations, over the electropolymerization reaction. Distortion of the conjugated backbone caused by steric interactions among substituents provokes a decrease of *p* orbitals overlap of thiophene rings and, consequently, a loss of conjugation that decreases its conductivity. These findings agree with the theoretical outcomes to be detailed below.

The different monomers cause modification in the kinetics and growth pattern of the polymerization process. Besides the analysis of nucleation and growth mechanism, characterization of this phenomenon was accomplished by recording SEM micrographs of the obtained deposits. From the potentiostatic transients, the global nucleation and growth mechanism (NGM) [33] can be established, that as demonstrated, in the case of polymeric electro-deposits is constituted by different contributions that participate simultaneous or successively, as a function of electrolysis time. In this case, deconvolution of the obtained transients indicates that the NGM can be represented by the following equation:

$$J = at[\exp(-bt^2)] + c[1 - \exp(-dt)] + et - 0,5[1 - -\exp(-ft^2)] \quad (6)$$

where the first term corresponds to instantaneous nucleation with bidimensional growth, NI2D, the second to instanta-

Table 2 Global electronic properties of 3′,4′-disubstituted 2,2′:5′,2″-terthiophene derivatives, calculated at B3LYP/6-311G** level. Energy is in kcal mol^{-1}, electronegativity (χ), hardness (η), softness (S), ionization potential (I) are in eV, dipole moment is given in Debye. α and β are the calculated torsion angles (in degrees)

	Energy	χ	η	S	$I = -\varepsilon_H$	Dipole moment (Db)	α	β
1a	1.21	3.64	1.90	0.53	5.53	1.37	34.1	34.1
1b	0.0	3.66	1.84	0.54	5.50	0.45	24.8	24.8
2a	0.0	3.91	1.98	0.51	5.89	1.52	43.1	43.1
2b	0.09	3.91	1.94	0.52	5.85	2.60	36.9	36.9
3a	0.51	3.79	1.92	0.52	5.71	1.09	42.2	35.8
3b	0.00	3.78	1.89	0.53	5.67	1.43	34.4	31.8
4a	0.30	3.55	1.89	0.53	5.44	1.88	35.6	35.6
4b	0.00	3.53	1.88	0.53	5.41	0.97	30.4	30.4
5a	0.00	4.58	1.86	0.54	6.44	5.70	41.3	41.3
5b	0.84	4.57	1.84	0.54	6.41	6.94	36.5	36.5

neous nucleation with diffusion controlled tridimensional growth, $NI3D_{diff}$, and the last term to instantaneous nucleation with charge transfer controlled growth, $NI3D_{ct}$. Deconvolved transient demonstrate that, on the one hand, the addition of the three contributions exactly fits the experimental transient, and on the other hand that at very short times NI2D, which stops after *ca*. 20 s, predominates.

Figure 3 shows micrographs of electro-deposits of polymers **2** and **3** obtained by the potentiodynamic method. As usually occurs, in the context of deposits obtained by cyclic voltammetry, more uniform surfaces are attained because during the potential sweep ordering of the deposit is favored. This is consistent with that predicted by the NGM prediction (Table 1) since just instantaneous nucleation was found, i.e., at the onset, a given number of nuclei is formed that grows as a function of electrolysis time, precluding further nuclei formation at higher times, which in another situation would lead to heterogeneous sizes. Consequently, an excellent agreement was found between the morphology predicted by NGM and that obtained by SEM, demonstrating that this sort of correlation is amenable to be performed and, at the same time, validating the proposed electropolymerization model [34].

Organic cells As for the incorporation of organic layers in solar cells fabrication, two techniques are employed, namely, blend (a layer tens of nanometers thick is deposited by spin-coating technique from a solution containing *p* and *n* type polymers) and bilayer (thin layers of organic semiconductors of both types of doping are deposited) [35]. Thus, the efficiency of the devices is related, among other factors, to the thickness of the constituent layers. All deposits that comprise the solar cell, except *p*-type polymers, can be controlled using the thermal evaporation technique while the thickness of polymer deposits is controlled by electrolysis time (potentiostatic method) or number of cycles (CV method) [36]. Solar cell preparation was achieved as follows: a glass support was coated with a layer of ZnO. Poly(3′,4′-dibromo-2,2′:5′,2″-terthiophene) (**2**), electron donor, was then deposited onto the ZnO film using electrochemical techniques, followed by 3,4-9,10-perylene tetracarboxylic dianhydride (PTCDA), LiF and Al deposition using special instrumentation and under high vacuum. The thickness was controlled by coupling a quartz crystal microbalance. Thus, the device configuration is as

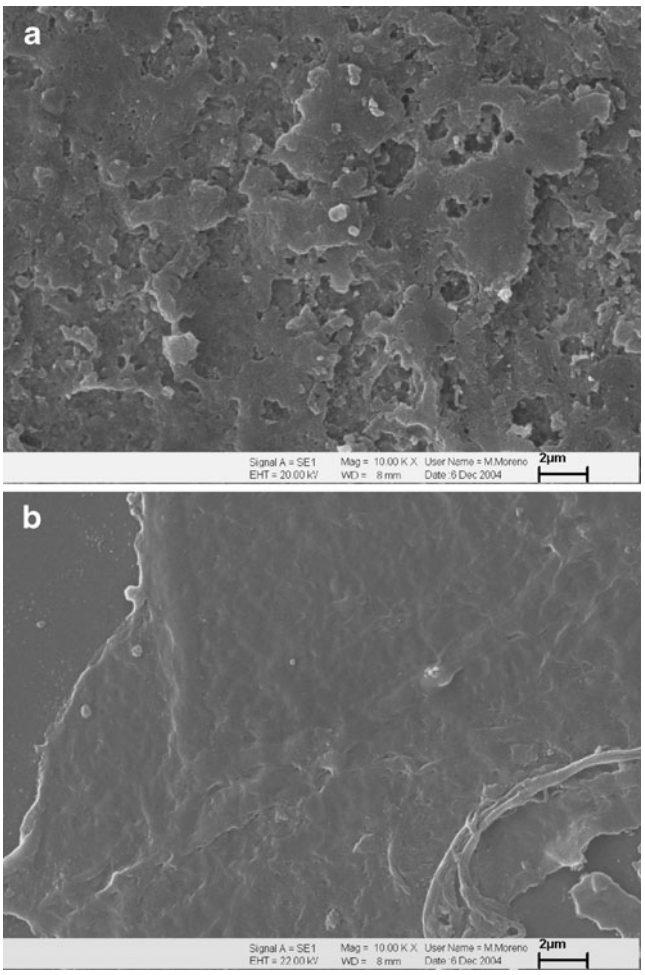

Fig. 3 Micrographs of deposits obtained by CV on Pt disc at 50 mV s^{-1}, (**a**) 3′,4′-dibromo-2,2′;5′,2″-terthiophene in CH_2Cl_2, (**b**) poly(3′,4′-biphenyl-2,2′;5′,2″-terthiophene) in CH_2Cl_2

follows: glass/ZnO (180 nm)/poly(3′,4′-dibromo-2,2′;5′,2″-terthiophene)/PTCDA (200 nm)/LiF (<15 nm)/Al (100 nm).

Thickness of the polymeric deposit was varied as a function of voltammetric cycles, as this technique afforded more homogeneous deposits, Fig. 3. It was found that thin polymer layers absorb in the visible and are electron acceptors. However, no photovoltaic effect was observed in solar cells using a polymer obtained by a small number of voltammetric cycles; instead, in 3′,4′-dibromo-2,2′:5′,2″-terthiophene the effect appeared after 20 cycles. As a result, a device with film thickness much larger than usually advised bearing photovoltaic characteristics and 0.06% efficiency was obtained, as shown in Fig. 4. The large thickness of the device probably accounts for the low efficiency obtained, even though, the deposit obtained by 20 cycles is still quite uniform and homogeneous. For the rest of deposits, responses were attained from the 10th cycle onward.

As for other deposits, such as poly(3′,4′-diphenyl-2,2′:5′,2″-terthiophene) and poly(3′-bromo, 4′-tienyl-2,2′:5′,2″-terthiophene) the devices displayed characteristics of organic light emitting diodes, OLEDs. The layer using 10 cycles for poly(3′,4′-diphenyl-2,2′:5′,2″-terthiophene) seems to be too thick and the diode only conduces after the application of 5 V and light shows up at *ca*. 8 V, Fig. 5 (light was measured using a photodiode).

The prepared devices were evaluated, using a simulator, to determine their efficiency in the fabrication of photovoltaic devices. As mentioned above, efficiency depends, among other factors, on the thickness of the constituent layers. In the absence of water in the working medium, these polymers can be deposited either by potentiostatic or potentiodynamic methods. In addition, morphology and film thickness can be controlled by the time of electrolysis or by the number of cycles which, as in other examples, confirms the feasibility of using electrochemical methods to deposit some layer(s) for the fabrication of optoelectronic devices [36].

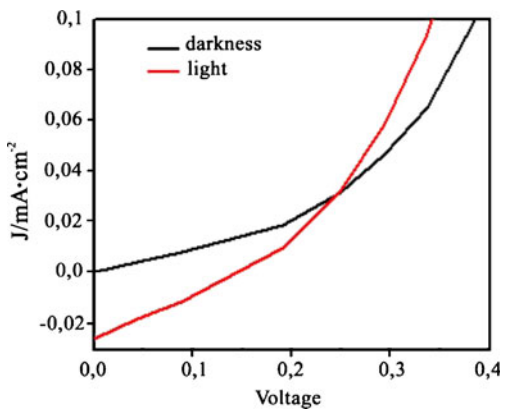

Fig. 4 Response of the device CG/ZnO/PTCDA/poly(3′,4′-dibromo-2,2′:5′,2″-trithiophene)/LiF/Al. Characteristic J=F(V)

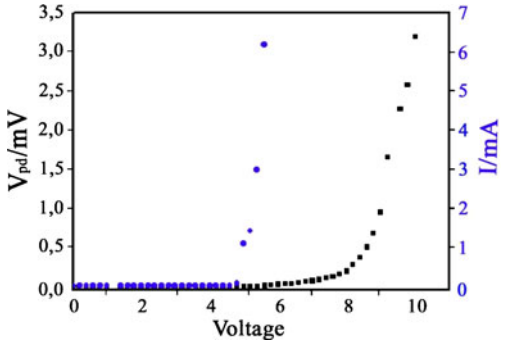

Fig. 5 Response of the CG/ZnO/PTCDA/poly(3′,4′-diphenyl-2,2′:5′,2″-terthiophene)/LiF/Al device

The maximum cell power was accomplished when light incidence angle is 90° with respect to its surface consequently, if the incidence angle is not 90°, the useful surface will decrease by an amount proportional to the cosine of the corresponding angle. Hence, the right panel orientation with respect to sun position during the different seasons of the year is quite important, according to the latitude of the installation. The low efficiency of the devices tested herein can be explained considering that *ca*. 57% of the luminous energy is reflected or becomes heat energy and that from the remaining 43%, most of it is given out as heat. The major difficulty is the risk of electrical rupture of the material caused by film defects. Besides, during operation the material must withstand the necessary voltage for its functioning. Table 1 lists the respective electrochemical parameters, oxidation potential (E_{ox}), NGM's and morphology for the synthesis of several compounds.

Theoretical results

Molecular structure and electronic density have been worked out for systems in Fig. 2 employing DFT (B3LYP/6-311G**) calculations. Computations showed, in general, geometries in which thiophene rings are non-coplanar with dihedral angles ranging from 24.8° to 43.1°, see Table 2. Among the isomers hard molecules present larger torsional angle and higher ionization potential. This structural feature accounts for the conductivity decrease at experimental level, consistent with a lower overlap between p_z orbitals of carbon atoms in adjacent rings, thereby a conjugation loss.

Figure 6 illustrates the HOMO densities of 2,2′:5′,2″-terthiophene (**1**) and 3′,4′-dinitro-2,2′:5′,2″-terthiophene (**5**) molecules showing that the most reactive sites for an electrophilic attack correspond to carbons adjacent to the sulfur atoms in the thiophene rings (within the red circle). Therefore, it is expected that polymerization occurs on these sites since, they present a considerable electronic density. However, the terminal sites should be favored

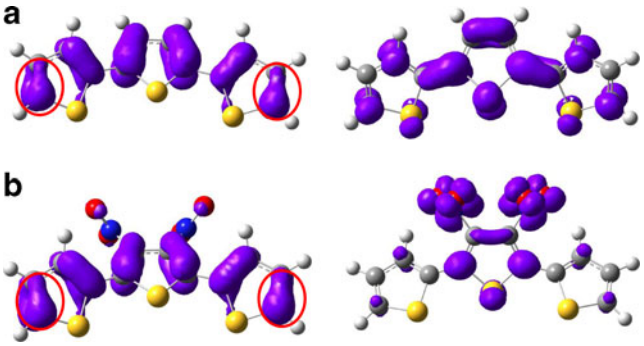

Fig. 6 Electronic density of the highest occupied and lowest unoccupied molecular orbitals, HOMO (left) and LUMO (right), respectively (**a**) 2,2′:5′,2″-terthiophene *cis*; (**b**) 3′,4′-dinitro-2,2′:5′,2″-terthiophene *cis*

because they present the lower steric hindrance, they should be the leading sites for polymerization.

All studied systems show HOMO and LUMO density over the rings. However, in 3′,4′-dinitro-2,2′:5′,2″-terthiophene *cis*, Fig. 6(b), the LUMO density is mainly localized over the nitro groups. Therefore the LUMO orbital may localize charge on the nitro groups region eventually preventing the electronic flow toward the aromatic rings, giving rise to disruption of the electronic conductivity. This accounts for the low conductivity found experimentally for this system. Notice that *cis* 3′,4′-dinitro-2,2′:5′,2″-tertiophene presents a high oxidation potential value (Table 1). This result has been theoretically supported by an ionization potential of 6.44 eV, which is slightly higher than that of the *trans* isomer, 6.41 eV, Table 2. These results agree well with the ^{1}H-NMR spectrum of 3′4′-dinitro-2,2′:5′,2″-terthiophene discussed above.

Computational characterization of the dual descriptor $\Delta f(r)$, has been performed for all molecules and the results are illustrated in Fig. 7 for representative systems **1** and **5**. In this figure the dual descriptor $\Delta f(r)$, notice that sites with $\Delta f(r)>0$ are electrophilic (purple), while sites with $\Delta f(r)<0$ are nucleophilic (green). As a rule, all systems presented $\Delta f(r)<0$ in carbons 4, 5 and 4″, 5″ (oxidation sites) revealing that these are nucleophilic and prospective oxidation sites. In addition, they are favored over the remaining nucleophilic sites because they lack the steric hindrance observed in sites close to the central ring substituents.

On the other hand, it has been experimentally found that the 3′,4′-dinitro-2,2′:5′,2″-terthiophene molecule exhibits poor conductivity and renders poor deposits, behavior that can be explained by means of the dual descriptor illustrated in Fig. 7. It was observed that, although the nucleophilic zone (green) still is on carbons 4, 5 and 4″, 5″ (oxidation sites), the major electrophilic concentration region (purple) is found on nitro groups (reduction sites), which makes this molecule exhibit an electrochemical behavior similar to nitrobenzene, where the reduction process prevails over the oxidation until the amine formation occurs. It is noteworthy that this system displayed the largest electronegative value, Table 2, which determines its electron acceptor capacity and susceptibility toward electrochemical reduction instead of the oxidative process necessary, essential for the polymerization to occur.

Conclusions

The results of the present investigation have demonstrated agreement between experimental and theoretical data obtained in the study of varied characteristics of some thiophene derivatives related to their capacity to conduct current.

Poly (3′,4′-biphenyl-2,2′:5′,2″-terthiophene) exhibited diode properties, but low capacity. Efficiency of the devices depends, among other factors, on the thickness of their constituent layers, glass/ZnO (180 nm)/PTCDA (200 nm)/polymer/LiF(<15 nm)/Al(100 nm). The thickness of all the above deposits but that of the polymer can be controlled by using the thermal evaporation technique. As for the polymer, its thickness can be regulated by the number of voltammetric cycles.

Chemical polymerization is not appropriate for this type of monomer, particularly when the polymer is intended for the fabrication of photovoltaic devices. By contrast, electropolymerization enables the obtention of deposits that can be tried as the electron donor active layer in electronic devices.

A good correlation was found between experimental j/t transients and those obtained by deconvolution. This is an indication that the mathematical models employed for metallic deposits are a good approximation for the study of this kind of electro-deposits. Good correlation between the morphology predicted by NGM's and to control by SEM was also encountered, which validates the methodology used to control the type of deposit to be obtained and the electropolymerization model previously proposed.

Substituents severely modify the electronic density and, hence, the reactivity of the thiophene ring. The steric effect helps to steer the polymerization toward lateral positions of the thiophene rings. In this context, the dual descriptor for chemical reactivity and selectivity has been found to be a

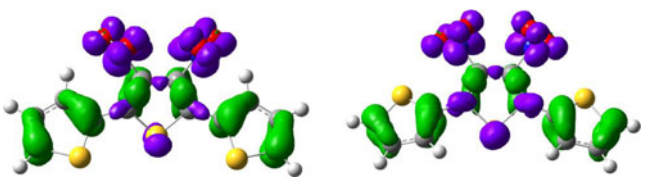

Fig. 7 Dual descriptor, $\Delta f(r)$, for 3′,4′-dinitro-2,2′:5′,2″-terthiophene *cis* (left) and *trans* (right). Electrophilic regions ($\Delta f(r)>0$) are in purple and nucleophilic regions ($\Delta f(r)<0$) are in green

nice indicator for predicting the specific sites able for reaction. Moreover, it explains correctly the observed polymerization pattern.

Acknowledgments Financial support from Programa Fondo de Financiamiento de Centros de Excelencia en Investigación (FONDAP) 11980002, Centro para la Investigación Interdisciplinaria Avanzada en Ciencias de los Materiales (CIMAT) and Fondo Nacional de Desarrollo Científico y Tecnológico (FONDECYT) through grants 1050953, 1060598, 11070197 and 1090460 is kindly acknowledged.

References

1. Díaz AF, Bargon J (1986) In: Skotheim TA (ed) Handbook of conducting polymers, vol 1. Dekker, New York, p 81
2. Roncali J (1992) Chem Rev 92:711–738
3. Shirakawa H, Louis EJ, McDiarmid AG, Chiang CK, Heeger AJ (1977) J Chem Soc Chem Commun 16:578–580
4. Chiang CK, Fincher CR, Park YW, Heeger AJ, Shirakawa H, Louis EJ, Gau SC, MacDiarmid AG (1977) Phys Rev Lett 39:1098–1101
5. Roncali J (1997) Chem Rev 97:173–206
6. Vélez JH, Díaz FR, Del Valle MA, Bernède JC, East GA (2006) J Appl Polym Sci 102:5314–5321
7. Vélez JH, Díaz FR, Del Valle MA, Soto JP, Bernède JC (2008) J Appl Polym Sci 109:1722–1729
8. Frommer JE, Chance RR (1998) In: Kroschwitz JI (ed) Electrical and electronic properties of polymers: A state of the art compendium. Wiley, New York
9. Chan HSO, Choon S (1998) Prog Polym Sci 23:1167–1231
10. Martín RE, Diederich F (1999) Angew Chem Int Ed 38:1350–1377
11. Yamamoto T (2002) Macromol Rapid Commun 23:583–606
12. Parr RG, Donnelly RA, Levy M, Palke WE (1978) J Chem Phys 68:3801–3807
13. Parr RG, Pearson RG (1983) J Am Chem Soc 105:7512–7516
14. Parr RG, Yang W (1984) J Am Chem Soc 106:4049–4050
15. Morell C, Grand A, Toro-Labbé A (2005) J Phys Chem A 109:205–212
16. Morell C, Grand A, Gutiérrez-Oliva S, Toro-Labbé A (2006) In: Toro-Labbé A (ed) A theoretical aspects of chemical reactivity, vol 19. Elsevier, Amsterdam, pp 101–117
17. Tamao K, Sumitani K, Kumada M (1972) J Am Chem Soc 94:4374–4376
18. Kumada M (1980) Pure Appl Chem 52:669–680
19. Casado AL, Espinet P (1998) J Am Chem Soc 120:8978–8985
20. East GA, Del Valle MA (2000) J Chem Ed 77:97
21. De Proft F, Geerlings P (1997) J Chem Phys 106:3270–3279
22. Koopmans TA (1933) Physica 1:104–113
23. Pearson RG (1985) J Am Chem Soc 107:6801–6806
24. Parr RG, Yang W (1989) Density functional theory of atoms and molecules. Oxford University Press, New York
25. Chattaraj PK, Pérez P, Zevallos J, Toro-Labbé A (2001) J Phys Chem A 105:4272–4283
26. Chattaraj PK, Gutiérrez-Oliva S, Jaque P, Toro-Labbé A (2003) Mol Phys 101:2841–2853
27. Frisch MJ, Trucks GW, Schlegel HB, Scuseria GE, Robb MA, Cheeseman JR, Zakrzewski VG, Montgomery JA, Stratmann RE, Burant JC, Dapprich S, Millam JM, Daniels AD, Kudin KN, Strain MC, Farkas O, Tomasi J, Barone V, Cossi M, Cammi R, Mennucci B, Pomelli C, Adamo C, Clifford S, Ochterski J, Petersson GA, Ayala PY, Cui Q, Morokuma K, Malick DK, Rabuck AD, Raghavachari K, Foresman JB, Cioslowski J, Ortiz JV, Stefanov BB, Liu G, Liashenko A, Piskorz P, Komaromi I, Gomperts R, Martin RL, Fox DJ, Keith T, Al-Laham MA, Peng CY, Nanayakkara A, Gonzalez C, Hallacombe M, Gill PMW, Johnson B, Chen W, Wong MW, Andres JL, Gonzalez C, Head-Gordon M, Replogle ES, Pople JA (2003) Gaussian03. Gaussian Inc, Pittsburgh
28. Becke AD (1992) J Chem Phys 96:2155–2160
29. Becke AD (1993) J Chem Phys 98:5648–5652
30. Lee H, Yang W, Parr RG (1998) Phys Rev B 37:785–789
31. Waltman RJ, Bargon J (1986) Can J Chem 64:76–95
32. Waltman RJ, Bargon J, Díaz AF (1983) J Phys Chem 87:1459–1463
33. Del Valle MA, Ugalde L, Del Pino F, Díaz FR, Bernède JC (2004) J Braz Chem Soc 15:272–276
34. Del Valle MA, Díaz FA, Bodini ME, Alfonso G, Soto GM, Borrego E (2005) Polym Int 54:526–532
35. Xue J, Rand BP, Uchida S, Forrest SR (2005) Adv Mater 17:66–71
36. Shaheen SE, Radspinner R, Peyghambarian N, Jabbour GE (2001) Appl Phys Lett 79:2996–2998
37. Schrebler R, Del Valle MA, Gómez H, Veas C, Córdova R (1995) J Electroanal Chem 380:219–227
38. Schrebler R, Grez P, Cury P, Veas C, Merino M, Gómez H, Córdova R, Del Valle MA (1997) J Electroanal Chem 430:77–90
39. Del Valle MA, Díaz FR, Bodini ME, Pizarro T, Córdova R, Gómez H, Schrebler R (1998) J Appl Electrochem 28:943–946
40. Del Valle MA, Cury P, Schrebler R (2002) Electrochim Acta 48:397–405
41. Del Valle MA, Ugalde L, Díaz FR, Bodini ME, Bernède JC, Chaillou A (2003) Polym Bull 51:55–62
42. Abé SY, Ugalde L, Del Valle MA, Trégouët Y, Bernède JC (2007) J Braz Chem Soc 18:601–606
43. Soto JP, Díaz FR, Del Valle MA, Vélez JH, East GA (2008) Appl Surf Sci 254:3489–3496
44. Del Valle MA, Camarada MB, Díaz FR, East GA (2008) E-Polymers 072:1–12